

Sensing Performance of Dual-Mode SAW Humidity Sensors on ScAlN/Si Using HfO₂ and SiO₂ Functionalization Layers

Monica NEDELICU^{1,2}, Dan VASILACHE¹, Florin NASTASE¹, Alexandra
NICOLOIU^{1,*}, Claudia NASTASE¹, Ioana ZDRU¹, George BOLDEIU¹, Adrian
DINESCU¹, and Alexandru MÜLLER¹

¹IMT-Bucharest, 32B(126A) Erou Iancu Nicolae Street, 077190 Voluntari, Ilfov, Romania

²Faculty of Electronics, Telecommunication and Information Technology, National University of Science
and Technology POLITEHNICA, 060042 Bucharest, Romania

¹ Email: monica.nedelcu@imt.ro, dan.vasilache@imt.ro,
florin.nastase@imt.ro, alexandra.nicoloiu@imt.ro*,
claudia.nastase@imt.ro, ioana.zdru@imt.ro, george.boldeiu@imt.ro,
adrian.dinescu@imt.ro, alexandru.muller@imt.ro

*Corresponding author

Abstract. This paper presents a comparative study of surface acoustic wave (SAW) humidity sensors fabricated on Sc_{0.3}Al_{0.7}N/Si, functionalized with HfO₂ and SiO₂ thin films, operating in both Rayleigh and Sezawa propagation modes. The paper describes the manufacturing of SAW humidity sensors by advanced nanolithographic processing tools and deposition methods of two different functionalization layers. The effect of HfO₂ and SiO₂ films on the resonance frequencies of the devices is analyzed for both propagation modes. The devices were characterized under controlled relative humidity conditions (20...90 %) by monitoring the resonance frequency shifts of both acoustic modes. Depending on the type of functionalization layer, the analyzed sensors exhibit distinct responses to humidity: the SAW sensors covered with HfO₂ show an increase of the resonance frequency with the relative humidity, while the SAW sensor having SiO₂ layer has an opposite response, the resonance frequency decreases with the increase of the humidity. This contrasting behavior is explained by the sensing mechanism that becomes dominant in each case: the stiffening effect for HfO₂ and the mass loading effect for SiO₂. The high values obtained for the humidity sensitivities confirm the advantage of SAW sensors manufacturing on III-Nitride/Si layered structures, allowing an increase of the resonance frequencies above 5 GHz.

Key-words: HfO₂ thin films, humidity sensing, SAW, ScAlN, SiO₂ functionalization layer.

1. Introduction

Over the past few decades, surface acoustic wave (SAW) devices have been intensively used in a wide range of applications. These include their use as filters related to landline and mobile communication systems, as well as sensors for measuring various physical parameters (temperature, pressure, humidity, gas concentration, etc.) in harsh environmental conditions, where wireless data reading and battery-less operation is necessary. More recently, SAW/spin wave coupling is envisioned, targeting future applications connected to spintronics and quantum computing. For all these applications, SAW devices have been manufactured mostly on bulk non-semiconductor piezoelectric materials (such as quartz, lithium niobate, lithium tantalate, etc.), which have very good piezoelectric properties and electromechanical coupling coefficient (k_{eff}^2). Given that the operating frequency of these SAW devices is usually limited to maximum 2...2.5 GHz, high order harmonics should be employed.

An increase of the resonance frequency of the SAW resonators, up to 5 GHz or more, is demanded for filters for 5G and 6G applications as well as for high sensitivity sensors, as the sensitivity is proportional to the resonance frequency (for temperature and pressure sensors) and to the square of the resonance frequency (for gas and humidity sensors). Also, the ferromagnetic resonance, which must fit the SAW resonance frequency in case of SAW/spin wave coupling, exceeds 2 GHz in most cases.

A reliable alternative to obtain higher resonance frequencies for the SAW devices consists in the use of compound semiconductors deposited or grown on different substrates, (such as GaN/SiC, GaN/sapphire, GaN/Si, AlN/Si and, very recently, $Sc_xAl_{1-x}N/Si$). Such III-Nitride based layered structures allow the fabrication of good quality SAW resonators operating at frequencies exceeding 3 GHz [1–3].

ScAlN is a novel CMOS compatible material and a great candidate for acoustic devices fabrication, due to its excellent piezoelectric properties: high phase velocity, enhanced electromechanical coupling coefficient, k_{eff}^2 , and high values of the piezoelectric constants [4–6]. ScAlN is more sensitive to surface changes due to its very high electromechanical coupling.

In layered piezoelectric structures such as ScAlN/Si, higher-order acoustic modes, including Sezawa mode [7], can be simultaneously excited together with the fundamental Rayleigh mode. Sezawa mode exhibits different penetration depth, which can significantly influence the interaction with the sensitive layer and, consequently, the sensing performance.

In sensor applications, a SAW device uses the propagation changes that occur due to the perturbation. Because most of the wave energy is concentrated on the SAW device surface, within one wavelength, any physical or chemical surface perturbations on the sensing films will have a significant impact on the propagating wave. An important element in gas and humidity sensors is represented by the functionalization layer which has the role to ensure a good and selective adsorption of the analyzed gas.

SiO_2 is of significant interest as functionalization layer for humidity sensors due to its hydrophilic properties, low cost, and versatile synthesis methods. SAW humidity sensors, using SiO_2 functionalization film synthesized by different methods, such as magnetron sputtering, physical vapor deposition, sol-gel, have been reported [8–10]. By adsorbing water molecules

from the air, the thin, porous SiO₂ functionalization layer induces a mass-dependent resonant frequency shift. The efficiency of this response is heavily influenced by the porosity and thickness of the SiO₂ film [10].

Hafnium oxide (HfO₂) has attracted attention in recent years due to its potential as a functional material in sensing applications, including humidity detection. Zhang et al. [11] showed that hafnia-based thin films modulate their ferroelectric properties under humidity, and Wang et al. [12] developed a humidity sensor based on porous silicon coated with HfO₂ thin film with improved sensing characteristics.

The sensing performance of SAW humidity sensors is strongly influenced by the properties of the functionalization layer. While SiO₂ has been widely used due to its stability and reproducibility, high-k dielectric materials such as HfO₂ offer increased sensing capability and stronger acoustic interaction. The presence of HfO₂ enhances this interaction due to its high density and stiffness. Consequently, it affects the SAW acoustic impedance by modifying the stiffness of the layer at surface, through water adsorption.

SAW humidity sensors are mostly manufactured on classical piezoelectric substrates. Lately, a quartz SAW sensor with Graphene oxide/TiO₂ coating film having a resonance frequency of 433.92 MHz and a sensitivity of ~14 kHz/% RH, was reported [13].

The experimental humidity sensing performance of the Sc_{0.3}Al_{0.7}N/Si SAW sensor with 58 nm HfO₂ sensitive layer, operating in Rayleigh mode, has been previously reported by the authors [14]. This article extends our previous work [14], “SAW humidity sensors manufactured on ScAlN/Si using HfO₂ sensing layer” (M. Nedelcu et al.). The present manuscript provides significant new contributions, including: (i) additional experimental measurements and sensitivity analysis for the Sezawa propagation mode of SAW sensors with HfO₂ functionalization layer and for both propagation modes, Rayleigh and Sezawa, for the SAW humidity sensor with SiO₂ functionalization layer, and (ii) a comparative performance analysis on the sensitivity of SAW humidity sensors on ScAlN/Si with HfO₂ and SiO₂ functionalization layers.

This paper is structured as follows: Section 1 presents an introduction regarding the applications of SAW devices, highlighting the SAW humidity sensors. Section 2 describes the fabrication process of the SAW sensors. Section 3 presents the on-wafer characterization, revealing the dual-mode operation of the SAW sensors, and introduces the experimental setup. Section 4 reviews the sensing mechanism, presents the frequency responses in the humidity range and analyses the results. Finally, Section 5 concludes on the obtained sensitivity values and the behavior of SAW humidity sensors.

2. Fabrication of the SAW Sensors

One-port SAW devices on ScAlN/Si layered structure were fabricated. The Sc_{0.3}Al_{0.7}N piezoelectric layer was deposited by Pulse Laser Deposition techniques by Solmates Nederlands, (currently Lam Research) on high resistivity Si substrates.

The fabrication process required the use of 3 photolithographic masks and one Electron Beam Lithography (EBL) process, in four steps, as follows: (i) first, the Coplanar Waveguide (CPW) line (~10/90 nm Ti/Au) was defined; (ii) the next step consisted in the fabrication of the IDT area, with the electrodes width equal to the distance between two consecutive electrodes, of 170 nm ($\lambda = 680$ nm). For this, an EBL process was used; to manufacture the IDTs, the metallization was Ti/Au (5/45 nm); (iii) next, an overlayer with a thickness of ~250 nm was deposited over the CPW line, to ensure the connection between the IDTs and the CPW line, and also to reduce

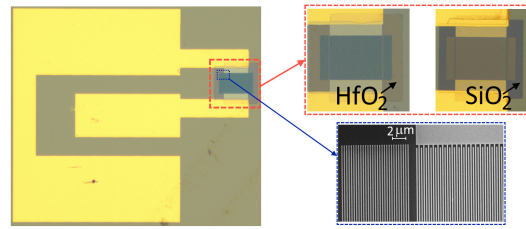


Fig. 1. Optical image of the fabricated SAW sensors; inset magnifying the IDT covered by HfO_2 or SiO_2 layer (up) and a SEM image of the IDT and reflectors (down).

the losses; (iv) in the last step the functionalization layer was deposited over the IDTs; the wafer was divided into two pieces: 58 nm HfO_2 layer was deposited on one piece by Atomic Layer Deposition (ALD) technique and, on the other one, 100 nm SiO_2 thin film using RF sputtering. The SAW structures were fabricated with two different IDT geometries, having different number of electrodes pairs: 112 pairs (sensor A) and 150 pairs (sensor B), respectively.

All fabrication steps, including lithography, metallization, HfO_2 and SiO_2 deposition, were carried out under identical technological conditions to ensure a consistent comparison between devices. The optical image of manufactured SAW sensor structure (B type) having HfO_2 or SiO_2 functionalization layer is shown in Fig. 1.

3. Characterization

The SAW devices were designed to support dual-mode operation. Rayleigh and Sezawa acoustic modes were first evidenced by on-wafer measurements at room temperature (RT), outside the climatic chamber, before and after the functionalization layers deposition. On-wafer measurements were performed with a VNA 37397D Vector Network Analyzer (Anritsu). The acoustic modes were identified based on their phase velocity and frequency response characteristics. The first resonance corresponds to the fundamental Rayleigh mode, while the second resonance is attributed to the Sezawa mode. The effect of HfO_2 deposition on the resonance frequencies and their magnitude, for both Rayleigh and Sezawa modes is presented in Fig. 2a,b.

A significant decrease in the resonance frequencies for both Rayleigh (from 5.8 GHz to 4.68 GHz) and Sezawa (from 8.2 GHz to 6.94 GHz) modes was observed in the S_{11} response, after HfO_2 deposition, due to the introduced mass loading effect (Fig. 2a,b). For 58 nm HfO_2 , the Sezawa mode becomes significantly attenuated. S_{11} parameters for the SAW device with SiO_2 functionalization layer are presented in Fig. 3 for both propagation modes and compared to the initial measurements performed on the same SAW device before SiO_2 layer deposition. SiO_2 functionalization layer deposition on the IDTs area also leads to a decrease of the resonance frequencies, for both Rayleigh (from 5.77 GHz to 5.63 GHz) and Sezawa (from 8.22 GHz to 8.13 GHz) modes. In this case, the shift in the resonance frequencies is smaller than that observed for the HfO_2 thin film. HfO_2 is denser ($\rho_{\text{HfO}_2} \approx 8.98 \text{ g/cm}^3$) than SiO_2 ($\rho_{\text{SiO}_2} \approx 2.20 \text{ g/cm}^3$), and its deposition significantly increases SAW devices mass loading.

After the deposition of the HfO_2 or SiO_2 functionalization layers, the SAW devices were characterized as humidity sensors. Humidity measurements were performed on both sensors, A and B, in the case of HfO_2 functionalization layer, while for SiO_2 sensitive film we analyzed the behavior of sensor B. The humidity response was evaluated using a controlled environmental

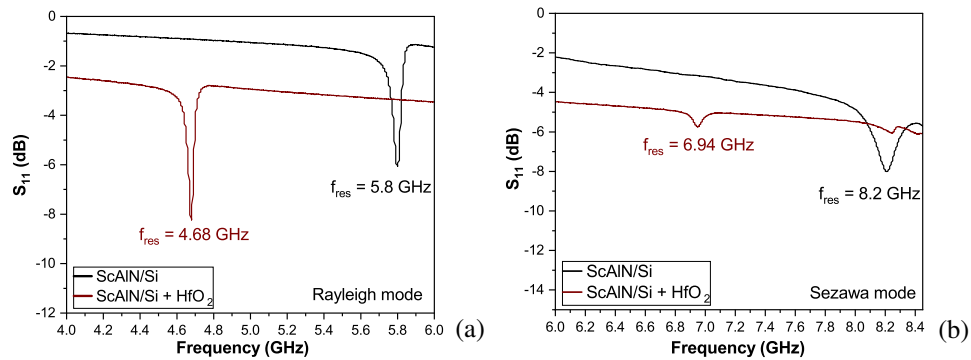


Fig. 2. S_{11} parameter of the SAW devices emphasizing the resonance frequency change after HfO_2 deposition, for Rayleigh (a) and Sezawa (b) modes.

chamber. Relative humidity was varied between 20% and 90% RH at a constant temperature of 30 °C. Measurements were performed in an ACS climatic chamber, model AV6005, 610 L, from Angelantoni Test Technologies Italy, which can control the temperature between -40...+180 °C and humidity in the range 10...95% RH. In Fig. 4 is presented the schematic of the experimental set-up for humidity measurements including the mounting assembly for SAW sensors.

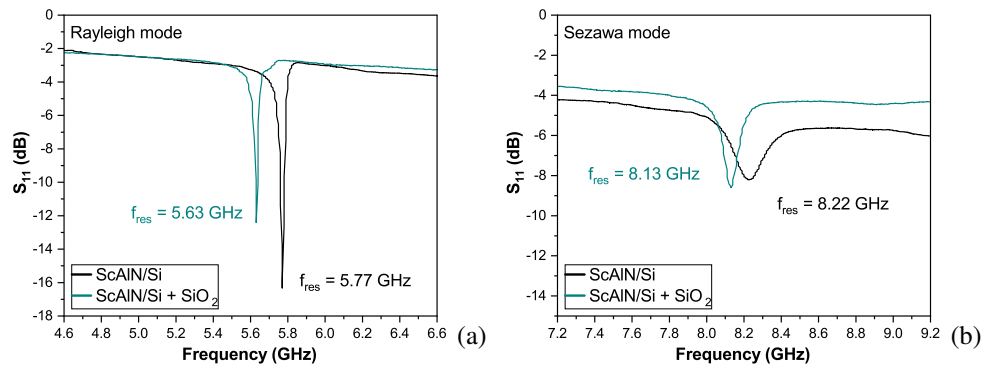


Fig. 3. S_{11} parameter of the SAW devices emphasizing the resonance frequency change after SiO_2 deposition, for Rayleigh (a) and Sezawa (b) modes.

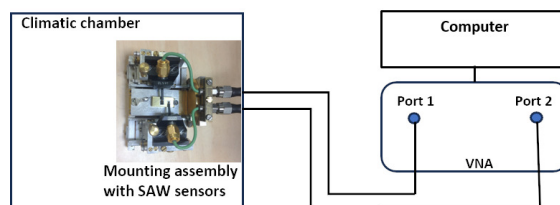


Fig. 4. Experimental set-up for the humidity measurements of the SAW sensors.

4. Results and Discussion

4.1. Humidity sensing mechanism

The resonance frequency of a surface acoustic wave (SAW) device is defined as $f_0 = v_0/\lambda_{ac}$, where v_0 is the acoustic phase velocity and λ_{ac} is the acoustic wavelength fixed by the IDT geometry. For small perturbations induced by a thin sensitive film, the relative frequency shift is directly related to the relative velocity variation in terms of

$$\frac{\Delta f}{f_0} = \frac{\Delta v}{v_0} \quad (1)$$

Considering a thin acoustic, non-piezoelectric, and isotropic layer with thickness $h \ll \lambda_{ac}$, deposited over a SAW device with wavelength λ_{ac} , phase velocity v_0 and resonance frequency f_0 , Wohltjen expressed the relative velocity variation, due to changes in the mass and stiffness of the layer as follows [15]:

$$\frac{\Delta v}{v_0} = -C_m f_0 h \Delta \rho + C_e f_0 h \Delta \left[\frac{4\mu}{v_0^2} \left(\frac{\lambda + \mu}{\lambda + 2\mu} \right) \right] \quad (2)$$

In equation (2), C_m and C_e are the sensitivity coefficients of the substrate connected to mass loading and elasticity [15], $h\Delta\rho$ is the mass per unit area change, μ , λ are Lamé constants of the film with thickness h . Equation (2) can be rewritten as:

$$\frac{\Delta f}{f_0} = \frac{\Delta v}{v_0} = -C_m f_0 \frac{\Delta m}{A} + 4C_e \frac{f_0}{v_0^2} h \Delta G' \quad (3)$$

and

$$\Delta f = -C_m f_0^2 \frac{\Delta m}{A} + 4C_e \frac{f_0^2}{v_0^2} h \Delta G' \quad (4)$$

where $\lambda = B - 2G/3$, B is the bulk modulus of the film, $\mu = G$ is the shear modulus and G' is the real part of G and $\Delta m/A$ represents the surface mass density variation.

The first term in equation (4) represents the inertial loading due to adsorbed mass. The absolute frequency shift becomes $\Delta f_{mass} \propto -f_0^2 \Delta m/A$ and has as effect the decrease of the resonance frequency [16]. The second term in (4), the elastic loading, takes into account changes in the effective shear modulus of the functionalization layer, $\Delta f_{elastic} \propto h \Delta G'$ and has as effect the increase of the resonance frequency.

During the humidity adsorption process there is a competition between the mass loading effect which leads to a negative frequency variation and the stiffening effect which causes an increase in the resonant frequency of the SAW humidity sensor:

$$\Delta f_{total} = -\Delta f_{mass} + \Delta f_{stiffness} \quad (5)$$

which will affect correspondingly the sensitivity which will be experimentally determined:

$$s = \frac{df}{dRH} \quad (6)$$

4.2. Frequency response in humidity range of Rayleigh and Sezawa modes

The SAW structures were mounted on a special carrier in order to perform relative humidity measurements in the climatic chamber. The relative humidity was changed from 20 to 90% with a step of 10% and the temperature was kept constant at 30°C. For each test point, the frequency change was recorded after a 30-minute waiting interval for the relative humidity to reach the equilibrium condition. The rate used for increasing humidity in the climatic chamber was 1%. Figs. 5a and 5b show the variation of the resonance frequency of the Rayleigh and Sezawa modes vs. RH for the SAW sensors A and B, having HfO₂ functionalization layer.

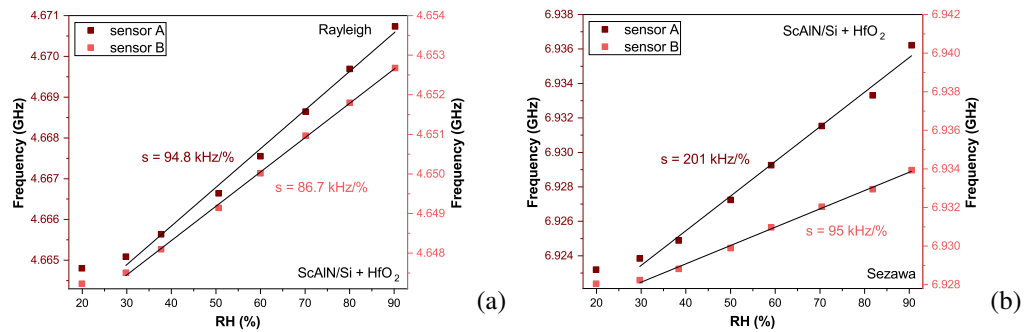


Fig. 5. Resonance frequency change vs. RH for SAW sensors A and B with HfO₂ functionalization layer, for Rayleigh (a) and Sezawa (b) modes.

The sensitivity, s , was determined from the slope of the linear fitting of frequency shift versus relative humidity. A linear variation of the resonance frequencies vs. RH is obtained on the RH range from 30% to 90% for both modes. Sensitivities of about 95 kHz/%RH for sensor A and 87 kHz/%RH for sensor B, in case of Rayleigh mode and about 201 kHz/%RH for sensor A and 95 kHz/%RH for sensor B for the Sezawa mode are determined. A consistent increase in resonant frequency was observed with increasing humidity for both SAW devices covered with HfO₂ indicating effective water molecule adsorption in the sensitive layers.

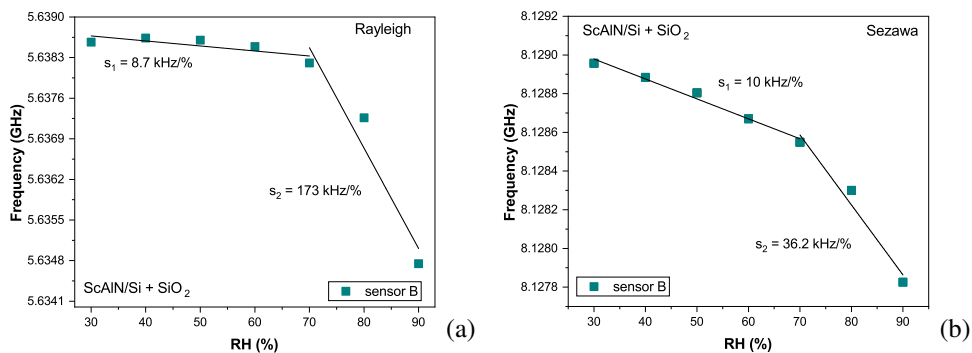


Fig. 6. Resonance frequency change vs. RH for SAW sensor B with SiO₂ functionalization layer; sensitivity determinations for Rayleigh (a) and Sezawa (b) modes.

The SAW device with SiO₂ functionalization layer was analyzed as humidity sensor, between 30 and 90% RH, with a step of 10%, at 30°C. Figs. 6a and 6b present the frequency shift of the Rayleigh mode and, respectively of the Sezawa mode vs. RH. In contrast with the SAW sensor with HfO₂ sensing film, the humidity sensors measurements for the SAW sensor with SiO₂ functionalization layer show a clear nonlinear behavior for both Rayleigh and Sezawa propagation modes. For Rayleigh mode the frequency shift was linearly fitted in 30 – 70% RH range with a humidity sensitivity about 9 kHz/%RH and between 70 and 90% the humidity sensitivity is 173 kHz/%RH. For Sezawa mode the relative humidity increases from 10 kHz/%RH for the first interval of relative humidity to 36 kHz/%RH for the second interval.

When we analyze the humidity response of SAW sensors with HfO₂ functionalization layer, there are two mechanisms that lead to the frequency change with the humidity: mass loading effect and stiffening effect. For some materials, the adsorption of water vapor causes the stiffening of molecules leading to an opposite contribution compared to mass loading effect. This behavior was reported for an AlN/Si-based SAW humidity sensor with a hydrophobic polymer film [17].

4.3. Results analysis

For the SAW structures covered with SiO₂, the resonance frequency decreases with increasing RH, and the dominant sensing mechanism is the mass loading effect.

In contrast to the most reported results, where the dominant sensing mechanism is the mass loading effect and the frequency decreases with increasing RH (for other piezoelectric substrates and coating layers [13]), for the HfO₂ functionalization layer, the resonance frequency increases with RH. This means that for the SAW sensors covered with HfO₂, the stiffening effect due to vapor adsorption is the main mechanism in the humidity sensor operation. The adsorbed water molecules lead to local stiffening at the surface of HfO₂ layer. This generates an increase of the Young's modulus and of the SAW velocity, leading to a positive frequency variation.

Although the stiffening effect appears to be the dominant mechanism, at low RH levels (20–30%), the sensitivity slope is noticeably reduced compared to higher humidity ranges. This behavior can be attributed to the weaker contribution of the elastic loading (stiffening) in this regime. At low humidity, the amount of adsorbed water is limited, leading to a relatively small variation in the shear modulus ($\Delta G'$) of the functionalization layer. The result is that the elastic loading effect becomes comparable in magnitude to the mass loading contribution. Since the two mechanisms contribute with different signs to the overall frequency shift, their partial compensation or reduced dominance results in a lower net sensitivity in this humidity interval.

The differences in sensitivity observed for sensors A and B can be explained by the different contributions of mass loading and elastic loading to the total frequency shift. As we concluded in equation (5), the overall frequency variation can be expressed as the superposition of two main effects: the elastic contribution (stiffening) which depends on the product $h\Delta G'$ being governed by the properties and thickness of coating layer, and the mass loading contribution that is directly influenced by the effective acoustic interaction area, determined by the IDT geometry. Since the mass loading term scales with the effective perturbed surface area, its magnitude increases with increasing IDT dimensions. Because the mass loading contribution appears with a negative sign in the frequency shift expression, equation (5), a larger IDT introduces a stronger subtractive term in the total response. As a result, even though the elastic contribution remains similar (being dependent on $h\Delta G'$), the increased mass loading term in larger IDTs reduces the net measurable sensitivity. Conversely, devices with smaller IDTs exhibit a reduced geometric mass-loading

contribution, allowing the elastic term to dominate more effectively, which leads to a higher overall sensitivity.

5. Conclusions

Humidity SAW sensors were manufactured on the emerging piezoelectric layered structure ScAlN/Si, using two different functionalization layers: the classical SiO₂ and less common for this type of application, HfO₂. The structures were characterized in the humidity range from 20 to 90% RH, at constant temperature, 30°C and a comparative experimental study was presented. The results demonstrate a strong dependence of the sensors behavior on the type of functionalization layer. The sensitivity determinations for the SAW structures covered with SiO₂ show a nonlinear variation of the resonance frequency vs. RH and the resonance frequency decreases with the increase of the relative humidity.

On the other hand, a very interesting behavior of the SAW humidity sensors with HfO₂ functionalization layer is noted: the main sensing mechanism is the stiffening effect and the resonance frequency increases when the humidity increases. This is in contrast to the behavior exhibited by the SAW structures covered with SiO₂ as well as to the most reported humidity sensors, where the mass loading effect is the dominant sensing mechanism. This might be explained by adsorbed water molecules that lead to local stiffening at the surface of the sensitive layer generating an increase in the effective Young's modulus of the HfO₂ layer.

Among the investigated devices, the sensor A, coated with 58 nm HfO₂, exhibited the highest sensitivity: 95 kHz/%RH for Rayleigh mode and 201 kHz/%RH for Sezawa mode. The experimentally observed higher sensitivity for smaller IDTs area can be attributed to a more favorable balance between elastic stiffening and geometry-dependent mass loading effects.

Acknowledgments. The authors of this paper acknowledge the support of the Romanian Ministry of Education and Research, under Contract 8N/2023 μ NanoEI - PN23070101 (Core Program) and of the European Project Horizon Europe HORIZON-CL4-2022-RESILIENCE-01 NANOMAT under Grant no. 101091433.

References

- [1] A. MÜLLER, G. KONSTANTINIDIS, I. GIANGU, V. BUICULESCU, A. DINESCU, A. STEFANESCU, A. STAVRINIDIS, G. STAVRINIDIS and A. ZIAEI, *GaN-based SAW structures resonating within the 5.4-8.5 GHz frequency range, for high sensitivity temperature sensors*, Proceedings of 2014 IEEE MTT-S International Microwave Symposium, Tampa, FL, USA, 2014, pp. 1–4.
- [2] G. BOLDEIU, G.E. PONCHAK, A. NICOLOIU, C. NASTASE, I. ZDRU, A. DINESCU and A. MÜLLER, *Investigation of temperature sensing capabilities of GaN/SiC and GaN/Sapphire surface acoustic wave devices*, IEEE Access **10**, 2021, pp. 741–752.
- [3] I. ZDRU, C. NASTASE, L.N. HESS, F. CIUBOTARIU, A. NICOLOIU, D. VASILACHE, M. DEKKERS, M. GEILEN, C. CIORNEI, G. BOLDEIU, A. DINESCU, C. ADELMANN, M. WEILER, P. PIRRO and A. MÜLLER, *A GHz operating CMOS compatible ScAlN based SAW resonator used for surface acoustic waves/spin waves coupling*, IEEE Electron Device Letters **43**(9), 2022, pp. 1551–1554.
- [4] B. LIN, Y. LIU, Y. CAI, J. ZHOU, Y. ZOU, Y. ZHANG, W. LIU and C. SUN, *A high Q value ScAlN/AlN-based SAW resonator for load sensing*, IEEE Transactions on Electron Devices **68**(10), 2021, pp. 5192–5197.

- [5] M. PARK, J. WANG, and A. ANSARI, *An 18 GHz AlScN film bulk acoustic wave resonator with epitaxial metal electrodes*, Proceedings of 22nd International Conference on Solid-State Sensors, Actuators and Microsystems (Transducers), Kyoto, Japan, 2023, pp. 1805–1808.
- [6] M. PARK, Z. HAO, R. DARGIS, A. CLARK and A. ANSARI, *Epitaxial aluminum scandium nitride super high frequency acoustic resonators*, Journal of Microelectromechanical Systems **29**(4), 2020, pp. 490–498.
- [7] A. MÜLLER, I. GIANGU, A. STAVRINIDIS, A. STEFANESCU, G. STAVRINIDIS, A. DINESCU, and G. KONSTANTINIDIS, *Sezawa propagation mode in GaN on Si surface acoustic wave type temperature sensor structures operating at GHz frequencies*, IEEE Electron Device Letters **36** (12), 2015, pp. 1299–1302.
- [8] X. YAN, C. LI, L. ZHAO, S. TIAN, Z. ZHANG, M. LI, H. LI, L. QIAN, X. GONG, Y. HUANG, T. HOU, H. BAI and B. YANG, *Surface acoustic wave relative humidity sensor based on sputtering SiO₂ film*, Surface and Interface Analyses **53**(10), 2021, pp. 867–875.
- [9] J. K. KWAN and J. C. SIT, *High sensitivity Love-wave humidity sensors using glancing angle deposited thin films*, Sensors and Actuators B: Chemical **173**, 2012, pp. 164–168.
- [10] Y. TANG, Z. LI, J. MA, L. WANG, J. YANG, B. DU, Q. YU and X. ZU, *Highly sensitive surface acoustic wave (SAW) humidity sensors based on sol–gel SiO₂ films: investigations on the sensing property and mechanism*, Sensors and Actuators B: Chemical **215**, 2015, pp. 283–291.
- [11] H. ZHANG, Y. SHEN, P. SHARMA, L. WANG, D. ZHANG, K. OOE, S. KOBAYASHI, Y. SHIMAKAWA, D. KAN and J. SEIDEL, *Humidity-driven modulation of ferroelectricity in hafnia–zirconia membranes*, Materials Horizons **12**, 2025, pp. 5762–5770.
- [12] Y. WANG and J.T.W. YEOW, *Humidity sensing of ordered macroporous silicon with HfO₂ thin-film surface coating*, IEEE Sensors Journal **9**(5), 2009, pp. 541–547.
- [13] Y. DOU, C. LI, W. LUO, L. QIAN, L. WANG, D. LI, H. LI and M. LI, *Surface acoustic wave relative humidity sensor based on GO/TiO₂ sensitive film*, Sensors and Actuators A: Physical **365**, 2024, pp. 1–9.
- [14] M. NEDELICU, D. VASILACHE, F. NASTASE, A. NICOLOIU, C. NASTASE, I. ZDRU, G. BOLD-EIU, A. DINESCU and A. MÜLLER, *SAW humidity sensors manufactured on ScAlN/Si using HfO₂ sensing layer*, Proceedings of 48th International Semiconductor Conference, Sinaia, Romania, 2025, pp. 105–108.
- [15] H. WOHLTJEN, *Mechanism of operation and design considerations for surface acoustic-wave device vapor sensors*, Sensors and Actuators **5**(4), 1984 pp. 307–325.
- [16] M. PASTERNAK, *Overtone oscillator for SAW gas detectors*, IEEE Sensors Journal **6**(6), 2006, pp. 1497–1501.
- [17] M. M. MEMON, Y. HONGYUAN, S. PAN, T. WANG and W. ZANG, *Surface acoustic wave humidity sensor based on hydrophobic polymer film*, Journal of Electronic Materials **51**(10), 2022, pp. 5627–5634.